



Ferrocenyl-containing silicone nanocomposites as materials for neuronal interfaces

Konstantin V. Deriabin^a, Sergey O. Kirichenko^a, Alexander V. Lopachev^b, Yuriy Sysoev^{c,d}, Pavel E. Musienko^{c,e,**}, Regina M. Islamova^{a,*}

^a Institute of Chemistry, St. Petersburg State University, 7/9 Universitetskaya Emb., St. Petersburg, 199034, Russia

^b Laboratory of Clinical and Experimental Neurochemistry, Research Center of Neurology, 80 Volokolamskoye Highway, Moscow, 125367, Russia

^c Pavlov Institute of Physiology RAS, 6 Makarov Emb., St. Petersburg, 199034, Russia

^d Department of Pharmacology and Clinical Pharmacology, St. Petersburg State Chemical and Pharmaceutical University, 14A Popova Str., 197376, Russia

^e Institute of Translational Biomedicine, St. Petersburg State University, 7/9 Universitetskaya Emb., St. Petersburg, 199034, Russia

ARTICLE INFO

Keywords:

Ferrocenyl-containing silicone rubbers
Nanocomposites
Cross-linking
Electrophysical properties
Neuronal implants

ABSTRACT

A synthetic method involving hydrosilylation reactions was developed to produce nanocomposites of elastic ferrocenyl-containing silicone rubber (EFSR) and multi-walled carbon nanotubes (MWCNT). The EFSR-MWCNT nanocomposites have a satisfactory elongation at break $\sim 80\%$, tensile strength (2.4 MPa), as well as electrical conductivity comparable to that of semiconductors ($7 \cdot 10^{-5} \text{ S} \cdot \text{cm}^{-1}$), all of which are necessary for application as neuronal implants. A novel prototype of a spinal cord neuronal interface based on EFSR-MWCNT was created as a prosthetic for impaired neuronal functions and to access spinal sensorimotor networks. Ferrocenyl groups in nanocomposites increase the charge injection that declines the risks of negative effects of electrical stimulation including nerve tissue damage.

1. Introduction

A considerable amount of research has been conducted on flexible electroconductive materials because of their promising biomedical applications as soft and electrochemical actuators [1–3], sensors and biosensors [1–7], tissue engineering materials [4,8], neuronal probes, prostheses and interfaces [9–17]. These materials are typically polymer nanocomposites with conductive fillers (carbon nanotubes or nanofibers, graphene, and metal nanoparticles) [12–16,18].

Elastic neuronal implants are the state-of-the-art in neuronal prosthetics. These flexible, thin electrical devices are placed directly on the surface of the spinal cord and brain to electrically and chemically stimulate nerve tissues [10]. These neuronal interfaces can be used to restore motor abilities in cases of paralysis from spinal cord injuries [11, 19]. Bearing in mind the considerable applied significance involved, it is challenging to develop novel materials for fabricating implants with a high level of biointegration and functionality.

Polydimethylsiloxanes (PDMS) are the most commonly used polymer matrixes in nanocomposites [4] (especially combined with multiwalled carbon nanotubes (MWCNT) [12,13,15,18] metal fillers [13,18], etc.) to

create elastic neuronal implants. PDMS possess superior flexibility, biocompatibility, film-forming ability, and resistance to chemical degradation [4,20].

We previously synthesized ferrocenyl-containing silicone rubbers (FSRs) [21] that have attracted considerable interest because of a unique combination of properties of typical PDMS [20,22,23] with redox activity [21]. The FSR has an electrical conductivity at the level of anti-static materials ($10^{-10} \text{ S} \cdot \text{cm}^{-1}$) [21], which is not enough for semiconductors. The MWCNT fillers allow increasing the electrical conductivity of polymer up to semiconductor [12]. Therefore, a challenging task is to obtain nanocomposites based on the FSR and MWCNT. The last one is promising for use as spinal cord neuronal implants since ferrocenyl groups increase the charge injection and thereby decline the risks of negative effects of electrical stimulation including nerve tissue damage. The main contribution of this study is the creation of a fundamentally new prototype of a spinal cord neuronal implant based on FSR with a smaller size in contrast to commercially available PDMS (DOWSIL™ Sylgard), which are used in the preparation of known neuronal implants [12,13,17].

Thus, we developed a novel synthetic method to produce a more

* Corresponding author. Institute of Chemistry, St. Petersburg University, 7/9 Universitetskaya Emb., St. Petersburg, 199034, Russian Federation.

** Corresponding author. Institute of Translational Biomedicine, St. Petersburg University, 7/9 Universitetskaya Emb., St. Petersburg, 199034, Russian Federation.

E-mail addresses: p.musienko@spbu.ru (P.E. Musienko), r.islamova@spbu.ru (R.M. Islamova).

elastic FSR (EFSR) by means of hydrosilylation reactions between vinylferrocene, polymethylhydrosiloxane (PMHS) and α,ω -di(trivinylsiloxy)polydimethylsiloxane (VPDMS) and fabricated flexible semi-conductive nanocomposites of EFSR-filled MWCNT; investigated the electrochemical and electrophysical characteristics of the nanocomposites; created a prototype of a spinal cord neuronal implant.

2. Experimental section

2.1. Materials

PMHS (number average molecular weight $M_n = 1700\text{--}3200$, viscosity 12–45 cSt, Abcr GmbH, Karlsruhe, Germany), and platinum(0)-1,3-divinyl-1,1,3,3-tetramethyldisiloxane complex solution 0.1 M in xylene (Abcr GmbH, Karlsruhe, Germany) were purchased from commercial suppliers and fully characterized by NMR spectroscopy before usage. VPDMS was synthesized via polymerization of octamethylcyclotetrasiloxane (98%, Abcr GmbH, Karlsruhe, Germany) using hexavinylsiloxane (95%, Gelest, US) as terminator and tetramethylammonium hydroxide (25 wt% in CH_3OH , Abcr GmbH, Karlsruhe, Germany) as an initiator (see Supplementary Material, section 1). Sylgard™ 184 Silicone Elastomer Kit (PDMS, Dow Corning, Midland, Michigan, USA) was used as received. CH_3OH (99%) was purchased from Vekton (St. Petersburg, Russia) and used without additional purification. CH_2Cl_2 (99%, Vekton, St. Petersburg, Russia) was distilled over P_2O_5 under argon prior to use. Toluene (99%) and THF (99%) were bought from Vekton (St. Petersburg, Russia) and freshly distilled over Na/benzophenone under argon before usage. Vinylferrocene was synthesized from ferrocene (98%, Shanghai Macklin Biochemical Co., Shanghai, China) by a three-step procedure (acylation, hydration, and dehydration) and purified on a column filled with neutral aluminum oxide via the published method [24].

Preparation of EFSR, PDMS films, semiconductive EFSR-MWCNT, and PDMS-MWCNT nanocomposites is described in detail in the Supplementary Material (section 1).

2.2. Methods

Tension tests were carried out at room temperature (RT) on a Shimadzu EZ-L-5kN universal testing machine: constant tensile speeds of 10 and 40 mm min^{-1} , at least five times for each series of polymer samples. Polymer films cut based on an ISO 527-type 1BA standard before the tension tests.

The electrical conductivity of the polysiloxane films was measured by broadband impedance spectrometry. The films were prepared as round plates with a fixed diameter of 20 mm and thickness in the range from 0.4 to 1.2 mm, and 10 nm carbon film thermal sputtering using Quorum Technologies Q150 TES sputter coater to ensure full surface electric contact. The samples were then placed between two round plate gold plated brass electrodes. The measurements of specific electrical conductivity were performed with a Novocontrol Alpha Broadband Dielectric spectrometer and a ZGS shielded sample cell providing constant clamping pressure to keep the sandwich structure. The temperature of the sample plate was controlled by evaporated liquid nitrogen flowing through gas heaters with accuracy higher than 0.1 °C. The films were allowed to reach thermal equilibrium before the conductivity experiment for at least 300 s at 25 °C. The measurement sequence included a frequency sweep (1000.0–0.1 Hz; 10 points per decade) with 30 mV signal amplitude. At least five measurements were conducted per frequency step followed by median specific resistance averaging.

Scanning electron microscopy (SEM) was carried out on a Carl Zeiss Supra 25 microscope. Prior to measurements, a film of the polymer was cut in two using a thin safety razor blade to examine the sample cross-section.

The electrochemical and capacitive properties of EFSR-MWCNT and PDMS-MWCNT electrodes in aqueous electrolytes were studied by cyclic

voltammetry (CV) and electrochemical impedance spectroscopy using a Solartron Analytical 1287A potentiostat/galvanostat in a three-electrode configuration (Ag|AgCl reference electrode, graphite counter electrode and designed working electrode with a circle working area with 5 mm diameter). Impedance spectroscopy measurements were carried out at a DC bias of 0 V with a sinusoidal signal of 10 mV in the frequency range from 0 to 1 kHz. The CV response of the EFSR-MWCNT and PDMS-MWCNT electrodes was measured in a buffered saline solution at potentials from -0.8 V to 1.2 V vs reference electrode and at various scan rates from 50 to 300 mV/s. The solution was prepared from chlorides (142 mM Na^+ , 5 mM K^+ , 2 mM Ca^{2+} , 1.5 mM Mg^{2+} , buffered with 50 mM TRIS (Vekton, Russia) [25]) and deionized water (18 M Ω m, Simplicity UV), sonicated for 15 min, and purged with a stream of argon at a rate of 100 mL min^{-1} at constant temperature (25 °C) for an additional 15 min. An appropriate amount of concentrated aqueous HCl was added to change pH to 7.40. During measurements, the solution was stirred at a speed of 100 rpm, and its temperature was fixed at 25.0 ± 0.1 °C on a hotplate with a built-in magnetic stirrer. To assess the electrochemical window of the solution, a potentiodynamic sweep was performed from -1.5 to $+1.5$ V (relative to the saturated Ag|AgCl electrode) with a scan rate of 10 mV/s. The potential range from -0.8 to $+1.2$ V was chosen for the above CV experiments based on this result. Finally, the charge storage capacity was determined as the integral over time from the cathode portion of the last CV cycle in each measurement.

2.3. Preparation of neuronal electrodes

Soft and elastic neuronal implants were created using metallic molds. Metallic forms for casting were obtained on a laser cutting machine FMark 20 NS (20 W), using AISI 321 stainless steel plates as mold blanks. Then, the surface of the steel plate was purified with isopropanol and dried in an oven at 100 °C for 10 min. The steel mold was coated with a thin layer of the universal silicone spray SILICOT (10 μm), in order to facilitate the removal of the implant from the mold. Next, a nanocomposite was pressed into the mold to form conductive tracks. The excess amount of the nanocomposite was scraped off the mold surface with a rubber spatula. The mold surface was then covered by the 80 μm layer of PDMS. A glass plate and height adjusters were used to obtain a flat PDMS surface with a predetermined thickness. Finally, the resulting structure was placed into the curing oven at 100 °C for 25 min. At the next stage, the cured PDMS layer, with conductive tracks of the EFSR-MWCNT nanocomposite, was removed from the mold and placed on a substrate with the conductive tracks facing up. The output parts of the conductive tracks were joined with steel wires, model AS 632 (diameter 0.1 mm), by using silver-based conductive glue. The resulting structure was covered with PDMS and placed in a curing oven at 100 °C for 35 min. A glass plate and height adjusters were used to obtain a flat PDMS surface and a predetermined layer thickness. The cured main part of the implant was removed from the substrate and the contact points were released from the PDMS coating using a micro knife. Wires exiting the implant were connected to the interface to stimulate and record neuronal tissue activity.

2.4. Biological testing of the neuronal interfaces made by EFSR-MWCNT

In order to study the toxic effects of the obtained materials, a culture of SH-SY5Y neuroblastoma cells was maintained in the presence of EFSR-MWCNT for 72 h. The culture of human neuroblastoma cells SH-SY5Y (ATCC, US) was cultivated in a 1:1 mixture of MEM medium with Earl's salts and glutamine (PanEco, Russia) and in F 12 culture medium without glutamine (PanEco, Russia) with the addition of 100 units/mL penicillin streptomycin (PanEco, Russia) and 10% fetal calf serum (Biosera, US). The culture was stored in a cell incubator at 37 °C, humidity 90%, 5% CO_2 (SHEL LAB, US). The medium was changed every 3 days. EFSR-MWCNT were attached to plates in which SH-SY5Y neuroblastoma cells were then cultured 0.5–1.0 mm above the cell layer.

After 72 h, we removed the samples and tested the culture viability of 8 control and MWCNT-treated experimental replicates. Cell viability was assessed using MTT assay in 96-well plates. The method is based on the reduction of yellow MTT (Russia, Dia M) with living cells to blue formazan. The optical density of the samples was measured with a Synergy H1 plate reader (BioTek, US).

To test the functionality of the fabricated neuronal electrodes, we used the classical decerebrated animal model [26,27] for electrophysiological experiments. All in-vivo tests were carried out in accordance with the requirements of Council Directive 2010/63EU of the European Parliament on the protection of animals used for experimental and other scientific purposes. Decerebration was performed at the precollicular-postmammillary level [26]. Laminectomy in the lumbosacral region was performed to access the spinal sensorimotor neuronal circuits by the EFSR-MWCNT-based neuronal electrode. Pairs of wires (FEP stainless steel insulated, AS632; Cooner Wire) were implanted into the hind limb muscles [26].

2.5. The method of analysis of myographic activity and evoked potentials

Simultaneous recording of electromyographic (EMG) activity in the multiple hind limb muscles during spinal cord stimulation showed the functionality of the manufactured neural electrodes to trigger spinal sensorimotor pathways. EMG signals were amplified by a differential amplifier (A-M Systems, model 1700) in the range from 10 Hz to 5 kHz and digitized at a frequency of 20 kHz using a National Instrument A/D board analog-to-digital converter. The analysis of EMG activity and evoked potentials was carried out using our own scripts for the Matlab program. In a decerebrated cat model, bipolar EMG electrodes (AS632 stainless steel wire; Cooner Wire, Chatsworth, CA, 0.2 mm diameter with Teflon coating) were implanted bilaterally into the gastrocnemius muscle (m. Gastrocnemius lateralis, Gast, ankle extensor, knee flexor) soleus muscle (m. Soleus (Sol), ankle extensor), iliopsoas (m. Iliapsoas (IP), hip flexor), and tibial muscle (m. tibialis (Tib), ankle flexor). In a study on a decerebrated rat model, EMG electrodes were implanted in a similar manner bilaterally into the gastrocnemius muscle, iliopsoas muscle, as well as into vastus lateralis muscle (m. Vastus lateralis (VL),

hip flexor).

3. Results and discussion

3.1. Preparation of EFSR-MWCNT nanocomposites

An EFSR polymer matrix of the EFSR-MWCNT nanocomposites was obtained via catalytic hydrosilylation reaction between PMHS, vinylferrocene, and high-molecular-weight VPDMS in a toluene solution (Fig. 1). Ultrasonic treatment was used to disperse MWCNT in the polymer matrix to prepare the EFSR-MWCNT nanocomposites (Fig. 1). An MWCNT concentration of 5 wt% was chosen to ensure that the resulting nanocomposite contained the maximum possible quantity of MWCNT. Nanocomposites with MWCNT concentrations >5 wt% resulted in coagulation and precipitation of MWCNT in the nanocomposites. MWCNT concentrations <5 wt% were insufficient to achieve an electrical resistivity in the 10^4 – 10^5 Ω -cm range, which is a prerequisite for use in neuronal implants [12]. MWCNT were added to a solution of freshly prepared non-cross-linked EFSR in toluene and mixed at RT for 10 min. The mixture was then concentrated, stirred in an ultrasonic bath for 7–8 min until the MWCNT dispersed completely, and poured into a polytetrafluoroethylene mold, followed by drying.

According to SEM (Fig. 2), the above-described method for obtaining nanocomposites makes it possible to homogeneously disperse MWCNT in a polysiloxane matrix, both in the case of EFSR-MWCNT and PDMS-MWCNT. SEM images confirm that an MWCNT concentration of 5 wt% (≈ 3 vol%) is the most optimal to prepare nanocomposites.

3.2. Tensile properties

EFSR is characterized by relatively high elongation at break (ϵ) $170 \pm 26\%$ and tensile strength (σ) of 3.5 ± 0.5 MPa (Fig. 3, a), as well as relatively low hysteresis (up to 14%) based on cyclic tensile-compression tests (Fig. 3, b). EFSR-MWCNT exhibits an ϵ of $80 \pm 10\%$ and a σ of 2.4 ± 0.3 MPa (Fig. 3, a). The Young's modulus (E) of EFSR-MWCNT (4.9 ± 0.6 MPa) is almost five times higher than that of EFSR ($E = 1.4 \pm 0.2$ MPa) in the low-strain region (up to 10%), and the

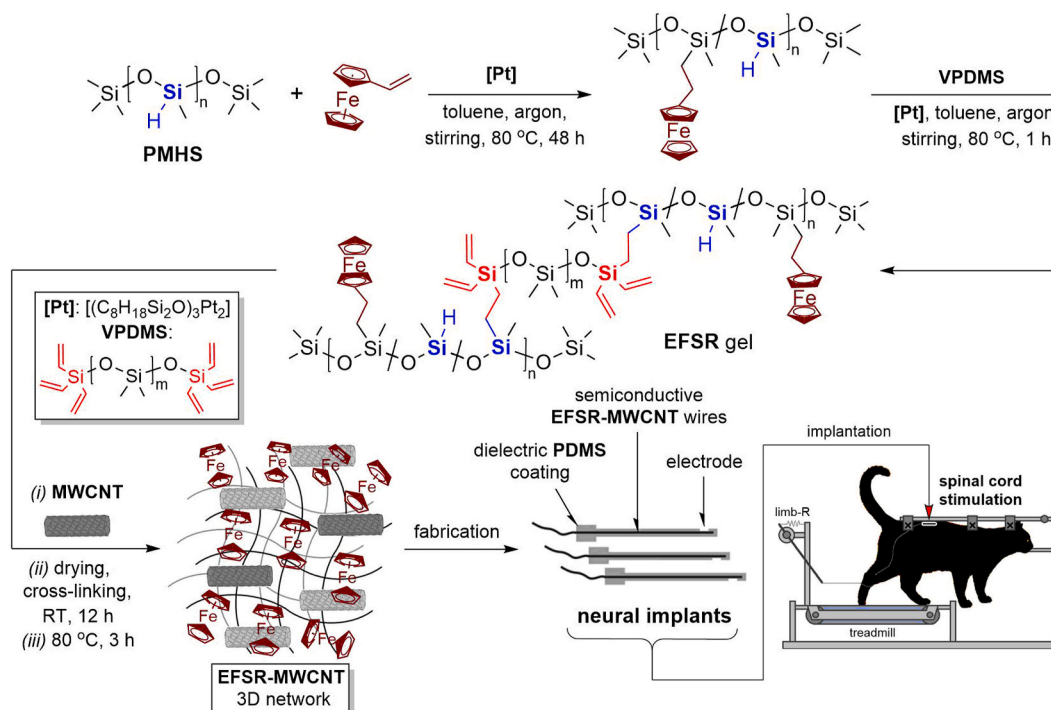


Fig. 1. Preparation of the EFSR-MWCNT nanocomposites and corresponding neuronal implants.

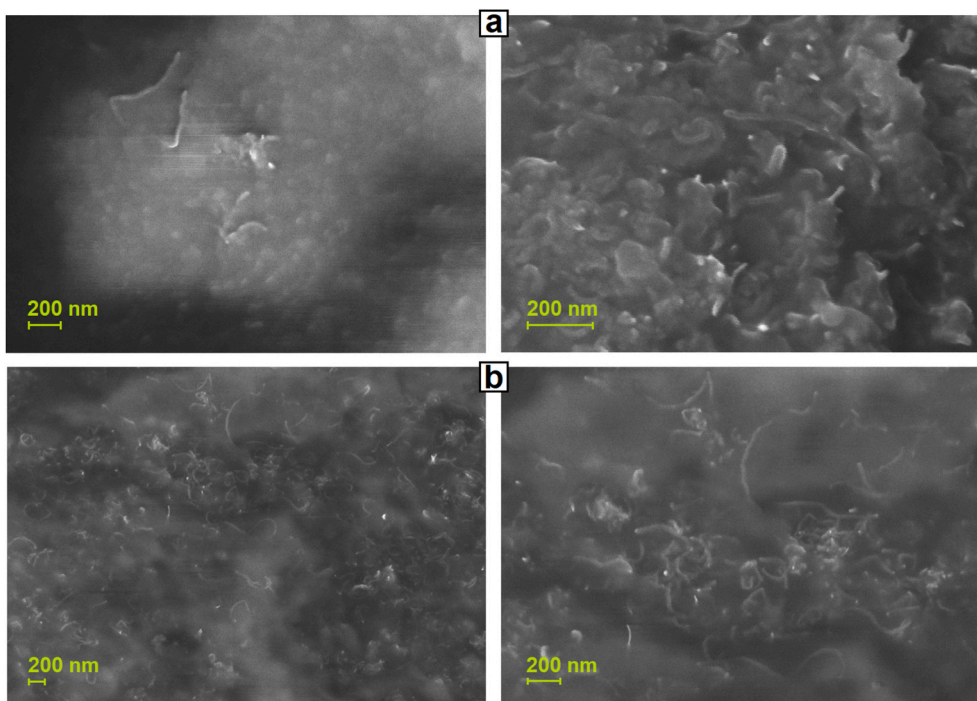


Fig. 2. SEM images of the EFSR-MWCNT (a) and PDMS-MWCNT (b) nanocomposites with MWCNT concentration of 5 wt%.

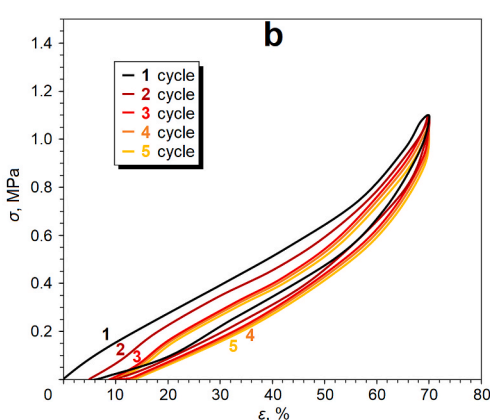
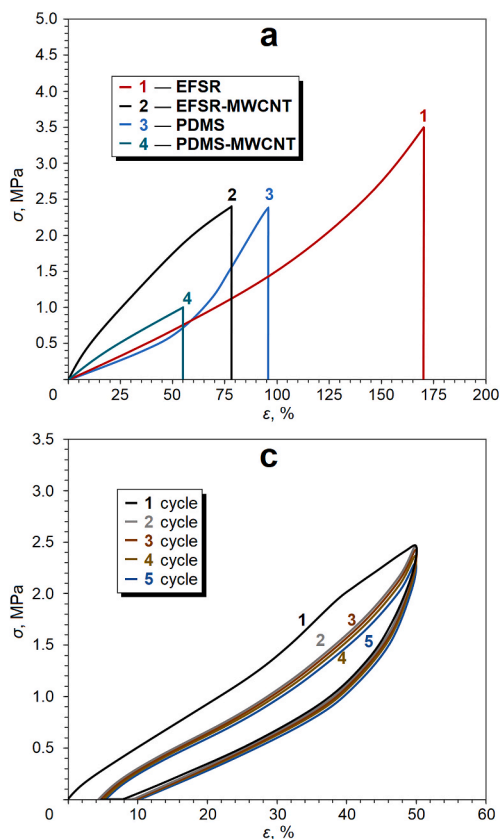
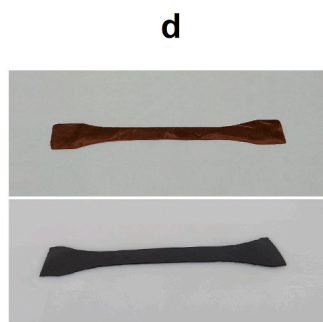


Fig. 3. a. Tensile properties of EFSR, PDMS, and the corresponding nanocomposites with 5 wt% MWCNT: stress-strain curves (the stretching speed is 40 mm min⁻¹); b. cyclic stress-strain tests by successive stretching (the stretching speed is 10 mm min⁻¹) for EFSR (70% strain); c. cyclic stress-strain tests by successive stretching (the stretching speed is 10 mm min⁻¹) for the EFSR-MWCNT nanocomposites (50% strain); d. photographs of the EFSR and EFSR-MWCNT films cut based on an ISO 527-type 1BA standard.



percentage of hysteresis based on tensile-compression cyclic tests is slightly lower for EFSR-MWCNT (approximately 10%) than for EFSR (Fig. 3, c). Moreover, the EFSR-MWCNT nanocomposites have mechanical properties almost two times superior to that of the model PDMS-MWCNT nanocomposites ($\epsilon = 55 \pm 5\%$, $\sigma = 1.0 \pm 0.1$ MPa, and

$E = 2.4 \pm 0.1$ MPa) but generally close to the model PDMS presented in Fig. 3, a.

Thus, the inclusion of ferrocenyl groups to a silicone matrix of nanocomposites leads to higher strength and Young's modulus since ferrocenyl substituents are bulky aromatic substituents compared to

methyl groups of PDMS.

3.3. Electrophysical and electrochemical properties

The frequency range of typical spinal stimulation pulse trains is approximately 1000 Hz; therefore, the electrical resistivity of EFSR and EFSR-MWCNT was investigated using broadband impedance spectroscopy in a frequency range from 1 MHz to 1 Hz (Fig. 4, a). PDMS without ferrocenyl fragments used in neuronal implants [12,13,17] (Sylgard™ 184), and the PDMS-MWCNT nanocomposites were tested as control samples. The electrical conductivity of the EFSR-MWCNT and PDMS-MWCNT nanocomposites exhibits a “metal-like” character [12] over almost the entire frequency range (the specific electrical conductivity of EFSR-MWCNT and PDMS-MWCNT is approximately $7 \cdot 10^{-5}$ and $3 \cdot 10^{-5} \text{ S}\cdot\text{cm}^{-1}$ at an electric current frequency of 1 Hz, respectively). The data are entirely similar to semiconductors and is c.a. 10^7 times higher than that of antistatic EFSR ($9.5 \cdot 10^{-12} \text{ S}\cdot\text{cm}^{-1}$ at 1 Hz), and c.a. 10^8 times higher than that of model dielectric PDMS ($7.5 \cdot 10^{-13} \text{ S}\cdot\text{cm}^{-1}$ at 1 Hz). This result indicates that the preferred transfer of charge carriers probably occurs *via* the formed carbon nanotube network. A percolation limit was inferred from the measured electrical conductivity of the nanocomposites with 0.1%–6% MWCNT (Fig. S2). The electrical conductivity increases sharply and abruptly beyond the percolation limit. Thus, the inclusion of ferrocenyl groups into the polymer matrix of nanocomposites leads to a 2-times slight increase of electrical conductivity.

In addition to the specific resistance measurements, the electrochemical properties of the obtained materials (Fig. 4, b), simulating a biological body fluid, were measured. Functional electrical stimulation requires a high localization of charge injection from the neuronal implant, which is achieved by minimizing the electrodes. However, a decrease in the geometric surface of the electrode leads to an increase in the density of the charge passing through it in a pulse to values exceeding safe limits. Using electroactive EFSR in the modified microelectrodes can lead to avoid tissue damage during stimulation. The ability of ferrocene to reversible one-electron oxidation makes it possible to achieve a high charge injection capacity without changing the electrode area (Table 1). Upon characterizing such microelectrodes, one of the main parameters of stability during stimulation is the charge storage capacity (CSC) — the amount of charge that the electrode can accumulate without undergoing irreversible Faraday reactions (Table 1). An extended electroactive range (“electrochemical window”) can be noted for EFSR-MWCNT in the cathode region (from -1.9 to $+2.0$ V) compared to PDMS-MWCNT (from -1.1 to $+1.3$ V) for neurostimulation. Thus, the ferrocenyl groups were found to increase the

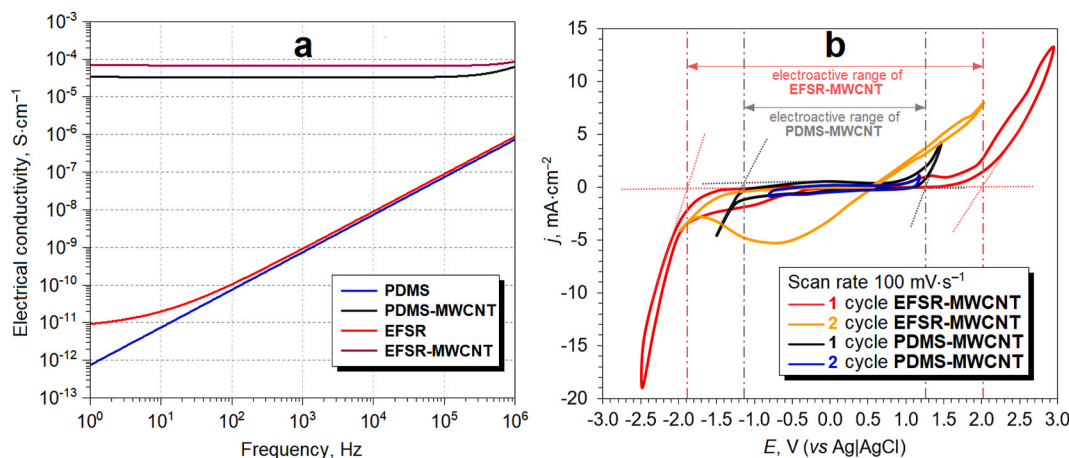


Fig. 4. a. Frequency dependence of specific electrical conductivity at 25 °C for PDMS, PDMS-MWCNT, EFSR, and EFSR-MWCNT; b. CV for determining the electrochemical range of an electrode taking the intersection of the linear fits of the CV curves (1st cycles, the crossing points of the dashed lines) and CV potential sweep 100 mV s^{-1} for the cathode CSC determination (2nd cycles).

Table 1
Cathode CSC of nanocomposites.

Scan rate, mV s^{-1}	CSC of EFSR-MWCNT	CSC of PDMS-MWCNT
50	$26.41 \text{ mC}\cdot\text{cm}^{-2}$ ($-1.0 \dots +0.8$ V)	$17.92 \text{ mC}\cdot\text{cm}^{-2}$ ($-0.4 \dots +1.0$ V)
100	$23.20 \text{ mC}\cdot\text{cm}^{-2}$ ($-1.0 \dots +0.8$ V)	$15.58 \text{ mC}\cdot\text{cm}^{-2}$ ($-0.4 \dots +1.0$ V)

charge injection for the same electrode area and led to 1.5 times higher CSC allowing to minimize the geometric surface of the electrode due to the ability of the ferrocenyl substituents to recharge during the application of voltage. These groups contribute to significantly reducing the potential negative effect of electrical stimulation, i.e., the risks of damage during electrical stimulation of nerve tissues.

3.4. Toxic effect of the EFSR-MWCNT nanocomposites on neuroblastoma cells

It was found that EFSR-MWCNT had a toxic effect on the cultured neuroblastoma cells (Fig. 5, a). Culture viability decreased by 86% compared to control cells. Data are presented as percent signals in the wells with intact control cells. Thus, as compared with nanocomposites based on commercially available silicones DOWSIL™ Sylgard, which are typically used in the preparation of known neural implants [12,13,17], EFSR-MWCNT should attract the attention of the biomedical community as flexible electroactive materials with potential antitumor activity [28–31] that can reduce the high risk of postoperative spinal cord tumor growth and canceration [32]. The material selective reaction of ferrocenyl-containing polysiloxanes with neuroblastomas may have resulted from the antitumor activity of ferrocene compounds [28–31].

3.5. Development of neuronal electrodes based on the EFSR-MWCNT nanocomposites

The novel electrically conductive EFSR-MWCNT nanocomposites were used to develop a prototype of neuronal electrodes for the first time (Fig. 5, b-i). The biological properties of electrode samples based on the electrically conductive EFSR-MWCNT were determined by performing *in vivo* experiments on laboratory animals in which the nanocomposites were used invasively (Fig. 5, b-f) and noninvasively (Fig. 5, g-i) to stimulate the spinal cord.

Invasive epidural electrical stimulation of the spinal cord was carried out by placing the EFSR-MWCNT-based electrodes (Fig. 5, b) on the

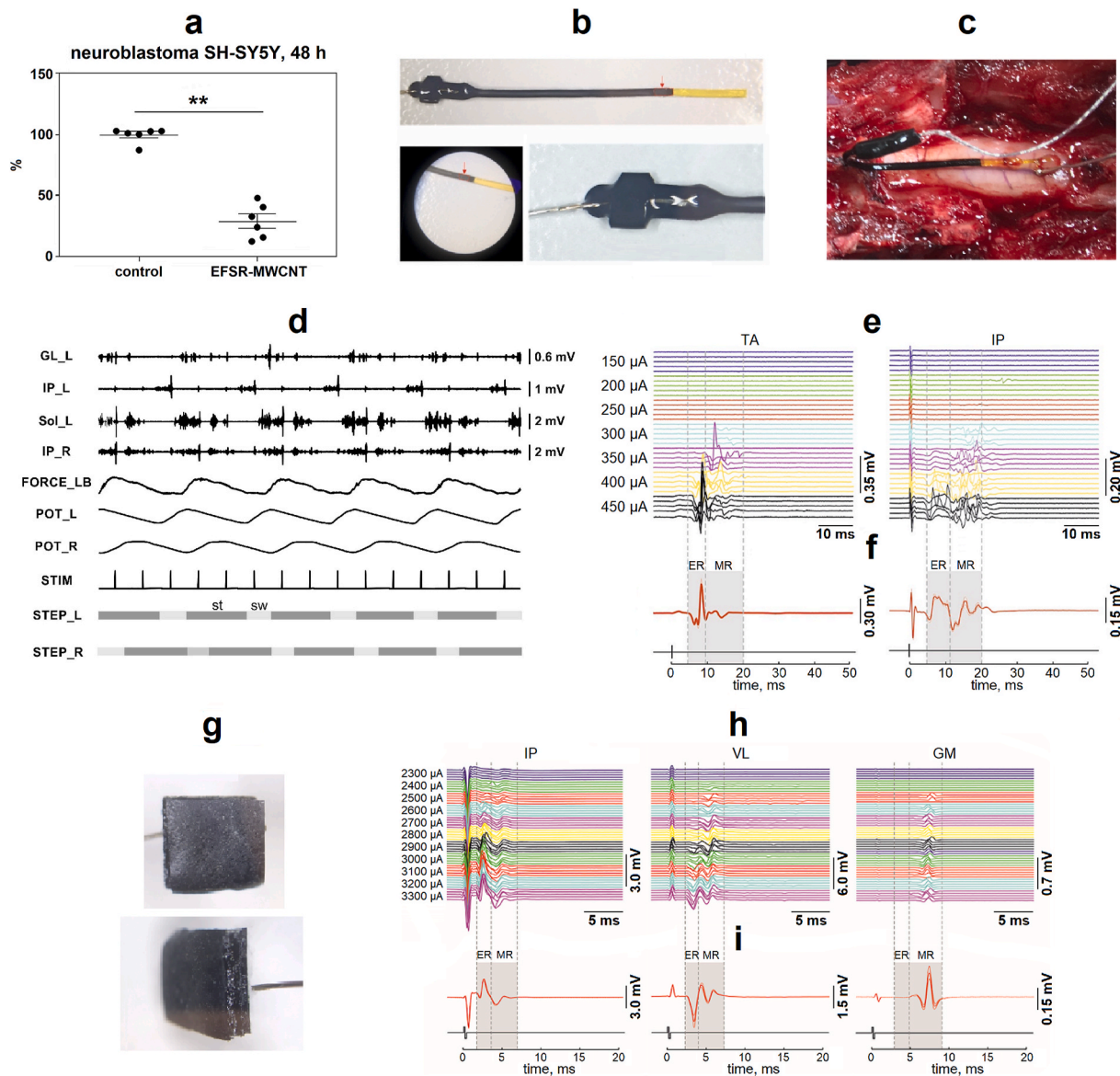


Fig. 5. **a.** Viability (%) of SH-SY5Y neuroblastoma cell culture incubated with or without EFSR-MWCNT for 72 h according to MTT-test. $N = 8$, ** – $p < 0.01$. **b.** Electrodes made of the electrically conductive EFSR-MWCNT nanocomposite for epidural electrical stimulation of the feline spinal cord, the red arrows mark the stimulated electrode after excision of the PDMS layer. **c.** An EFSR-MWCNT-based electrode was placed on the lumbar enlargement of a cat spinal cord. **d.** Kinematic and myographic signals of the muscles of the hind limbs of a decerebrated cat during locomotion evoked by epidural spinal cord stimulation with an EFSR-MWCNT electrode. GL gastrocnemius muscle, IP — iliopsoas muscle, Sol — soleus muscle, Force_{LB} — left leg support force, Pot_L and Pot_R — left and right paw potentiometer signals, STIM — stimulation channel; st (stance) and sw (swing) — phases of the support and transfer of the left and right paws during locomotion. **e.** Reflex recruitment in the tibial muscle (TA) and iliopsoas muscle (IP) by the epidural spinal cord (L7 spinal segment) stimulation at a frequency of 1 Hz with an EFSR-MWCNT electrode in decerebrated cat; averaged evoked potentials ($n = 5$) in TA and IP at maximum current (450 μA). **f.** Short-latency (ER) and mid-latency (MR) reflex responses are highlighted in gray. **g.** EFSR-MWCNT-based electrodes for transcutaneous electrical stimulation of the rat spinal cord. **h.** Reflex recruitment in the iliopsoas muscle (IP), vastus lateralis (VL) and gastrocnemius (GM) by the transcutaneous spinal cord (L2–L3 spinal segments) stimulation at a frequency of 1 Hz with an EFSR-MWCNT electrode in decerebrated rat; **i.** averaged evoked potentials ($n = 5$) IP, VL and GM at maximum current (3300 μA). Short-latency (ER) and medium-latency (MR) reflex responses are marked with a dotted line. (For interpretation of the references to colour in this figure legend, the reader is referred to the Web version of this article.)

surface of the lumbosacral enlargement (Fig. 5, c) to induce locomotor activity and reflex responses of the muscles of the hind limbs of cats (stimulation frequency: 5 and 1 Hz, stimulus duration: 0.3 ms, and current strength: 0–450 μA in 50-kA increments). An A-M Systems model 2100 stimulator was used in the experiment. Skin EFSR-MWCNT electrodes (Fig. 5, g) were used for noninvasive percutaneous stimulation of the rat spinal cord (stimulation frequency: 1 Hz, stimulus duration: 0.1 ms, and current: 0–3300 μA in 100- μA increments).

Epidural stimulation of the spinal cord with an EFSR-MWCNT-based electrode at a frequency of 5 Hz activated the spinal locomotor network

and initiated a well-coordinated cat walk along a treadmill (Fig. 5, d). An analysis of the locomotor activity of a decerebrated cat showed a clear correlation between the phases of support and transfer recorded by the potentiometers and the activity of the flexor and extensor muscles. The myographic signals showed the reciprocity of the ipsilateral flexors (IP_L) and extensors (Sol_L and GL_L), as well as the corresponding muscles of the left and right limbs (IP_L vs IP_R). Gradually increasing the single-pulse epidural stimulation (1 Hz, 100–450 μA) triggered specific sensorimotor pathways of the cat spinal cord (Fig. 5, e-f). Medium-latency responses (~10–12 ms) were recorded at low

stimulation thresholds and increasing the current strength produced short-latency waves (~3–5 ms) corresponding to the classic dynamics of sensory H-reflex suppression by the direct motor response (M-response) [33]. The data obtained showed the capacities of the EFSR-MWCNT-based neural electrodes to trigger specific sensorimotor pathways of the cat spinal cord.

Similar dynamics were observed for the electrical epidural stimulation of the spinal neuronal pathways of decerebrated rats by a skin EFSR-MWCNT-based electrode at the level of L2–L3 vertebrae as for the decerebrated cat model. A sensory mid-latency response (H-reflex) was generated at lower currents than for the M-response (Fig. 5, h-i). Increasing the amplitude of stimulation suppressed the sensory response from motor activity in the iliopsoas and vastus lateral muscles. Note that stimulation of these spinal cord segments only generated a sensory response in the gastrocnemius muscle. This feature may be associated with a caudal localization of the pools of motor neurons innervating this muscle [34,35].

3.6. Comparison between EFSR-MWCNT and PDMS-MWCNT nanocomposites

The reported EFSR-MWCNT and PDMS-MWCNT nanocomposites exhibit some differences: (i) the EFSR-MWCNT nanocomposites have higher charge injection (23.20–26.41 mC·cm⁻²) compared to the control PDMS-MWCNT samples (15.58–17.92 mC·cm⁻²) with the same electrode area that allow to minimize the geometric surface of the electrode; (ii) the EFSR-MWCNT nanocomposites have a broader “electrochemical window” (from -1.9 to +2.0 V) for neurostimulation compared to PDMS-MWCNT (from -1.1 to +1.3 V) and can significantly reduce operational risks (damage during neurostimulation); (iii) introducing ferrocenyl groups into the nanocomposites can lead to a 2-times slight increase of electrical conductivity of EFSR-MWCNT (7·10⁻⁵ S·cm⁻¹) compared to PDMS-MWCNT (3·10⁻⁵ S·cm⁻¹); (iv) a morphology of EFSR-MWCNT and PDMS-MWCNT is close; (v) mechanical parameters of EFSR-MWCNT (elongation at break ~80%, tensile strength 2.4 MPa, hysteresis ~10%, Young’s modulus 4.9 MPa) are almost twice more than that of the model PDMS-MWCNT nanocomposite; (vi) the EFSR-MWCNT nanocomposites have potential antitumor activity (toxic effect on the cultured neuroblastoma cells) compared to PDMS-MWCNT that can reduce the high risk of postoperative spinal cord tumor growth and canceration [32].

4. Conclusion

A synthetic method involving hydrosilylation reactions was developed to produce semiconductive, elastic and flexible EFSR-MWCNT nanocomposites. EFSR-MWCNT has good mechanical properties, as well as electrical conductivity comparable to that of semiconductors, all of which are necessary for application as neuronal implants. The ferrocenyl groups also increase the charge injection and “electrochemical window” for neurostimulation compared to PDMS-MWCNT that declines the risks of negative effects of electrical stimulation including nerve tissue damage.

The obtained EFSR-MWCNT nanocomposites were tested for use as novel neuronal implants and noninvasive neurointerfaces. The biological properties were determined, and functional efficiency was demonstrated for stimulating neuronal networks of the spinal cord, neuromodulating motor pools, registering the activity of neuronal pathways, and recovering locomotor capacities after paralysis.

Further studies on the EFSR-MWCNT nanocomposites and the design of corresponding novel optimized neuronal implants are currently underway in our scientific groups.

Contributor roles taxonomy

Konstantin V. Deriabin: Methodology, Validation, Investigation,

Writing – Original Draft, Visualization. **Sergey O. Kirichenko:** Validation, Investigation. **Alexander V. Lopachev:** Validation, Investigation. **Yuriy Sysoev:** Validation, Investigation. **Pavel E. Musienko:** Conceptualization, Validation, Resources, Writing – Review & Editing, Supervision. **Regina M. Islamova:** Conceptualization, Validation, Resources, Writing – Review & Editing, Supervision, Project administration, Funding acquisition.

Declaration of competing interest

The authors declare that they have no known competing financial interests or personal relationships that could have appeared to influence the work reported in this paper.

Acknowledgment

Financial support for the assessment of the mechanical and electrical properties of the synthesized ferrocenyl-containing silicone rubbers and composites was provided by the Russian Science Foundation (project № 20-19-00256). Financial support for the polymers synthesis was provided by the Russian Foundation for Basic Research (project № 18-33-20062 mol_a_ved). The infrastructure for the in vivo tests and analysis was provided by the St. Petersburg State University (project ID: 73025408). The physicochemical measurements were performed at the Magnetic Resonance Research Center, the Center for Innovative Technologies of Composite Nanomaterials, and Interdisciplinary Resource Centre for Nanotechnology (which are parts of the St. Petersburg State University). We thank K.P. Kotlyar (St. Petersburg Academic University) for conducting SEM measurements and O.V. Gorsky for technical assistance with electrode fabrication.

Appendix A. Supplementary data

Supplementary data to this article can be found online at <https://doi.org/10.1016/j.compositesb.2022.109838>.

References

- [1] Ilami M, Bagheri H, Ahmed R, Skowronek EO, Marvi H. Materials, actuators, and sensors for soft bioinspired robots. *Adv Mater* 2020;2003139. <https://doi.org/10.1002/adma.202003139>.
- [2] Chen D, Pei Q. Electronic muscles and skins: a review of soft sensors and actuators. *Chem Rev* 2017;117:11239–68. <https://doi.org/10.1021/acs.chemrev.7b00019>.
- [3] Wang K, Ouyang G, Chen X, Jakobsen H. Engineering electroactive dielectric elastomers for miniature electromechanical transducers. *Polym Rev* 2017;57:369–96. <https://doi.org/10.1080/15583724.2016.1268156>.
- [4] González Calderón JA, Contreras López D, Pérez E, Vallejo Montesinos J. Polysiloxanes as polymer matrices in biomedical engineering: their interesting properties as the reason for the use in medical sciences. *Polym Bull* 2020;77:2749–817. <https://doi.org/10.1007/s00289-019-02869-x>.
- [5] Wang L, Chen Y, Lin L, Wang H, Huang X, Xue H, et al. Highly stretchable, anti-corrosive and wearable strain sensors based on the PDMS/CNTs decorated elastomer nanofiber composite. *Chem Eng J* 2019;362:89–98. <https://doi.org/10.1016/j.cej.2019.01.014>.
- [6] Song P, Song J, Zhang Y. Stretchable conductor based on carbon nanotube/carbon black silicone rubber nanocomposites with highly mechanical, electrical properties and strain sensitivity. *Compos B Eng* 2020;191:107979. <https://doi.org/10.1016/j.compositesb.2020.107979>.
- [7] Bai L, Yan X, Feng B, Zheng J. Mechanically strong, healable, and reprocessable conductive carbon black/silicone elastomer nanocomposites based on dynamic imine bonds and sacrificial coordination bonds. *Compos B Eng* 2021;223:109123. <https://doi.org/10.1016/j.compositesb.2021.109123>.
- [8] Oh JY, Bao Z. Second skin enabled by advanced electronics. *Adv Sci* 2019;1900186. <https://doi.org/10.1002/advs.201900186>.
- [9] Yang M, Liang Y, Gui Q, Chen J, Liu Y. Electroactive biocompatible materials for nerve cell stimulation. *Mater Res Express* 2015;2:042001. <https://doi.org/10.1088/2053-1591/2/4/042001>.
- [10] Minev IR, Musienko P, Hirsch A, Barraud Q, Wenger N, Moraud EM, et al. Electronic dura mater for long-term multimodal neural interfaces. *Science* 2015;347:159–63. <https://doi.org/10.1126/science.1260318>.
- [11] Wenger N, Moraud E, Gandar J, Musienko P, Capogrosso M, Baud L, et al. Spatiotemporal neuromodulation therapies engaging muscle synergies improve motor control after spinal cord injury. *Nat Med* 2016;22:138–45. <https://doi.org/10.1038/nm.4025>.

- [12] Barshutina MN, Kirichenko SO, Wodolajski VA, Musienko PE. Mechanisms of electrical conductivity in CNT/silicone composites designed for neural interfacing. *Mater Lett* 2019;236:183–6. <https://doi.org/10.1016/j.matlet.2018.10.090>.
- [13] Voros J, Courtine G, Larmagnac A, Musienko P. Pdms-based stretchable multi-electrode and chemotrode array for epidural and subdural neuronal recording, electrical stimulation and drug delivery. 2018, US10130274B2.
- [14] Maghribi MN, Krulevitch PA, Courtney JD, Wilson TS, Hamilton JK, Benet WJ, et al. Stretchable polymer-based electronic device. *US7337012B2*; 2008.
- [15] Sridharan A, Kodibagkar V, Muthuswamy J. Penetrating microindentation of hyper-soft, conductive silicone neural interfaces in vivo reveals significantly lower mechanical stresses. *MRS Adv* 2019;4:2551–8. <https://doi.org/10.1557/adv.2019.356>.
- [16] Osmani B, Schiff H, Vogelsang K, Guzman R, Kristiansen PM, Crockett R, et al. Hierarchically structured polydimethylsiloxane films for ultra-soft neural interfaces. *Micro.Nano.Eng* 2020;7:100051. <https://doi.org/10.1016/j.mne.2020.100051>.
- [17] Afanasenkau D, Kalinina D, Lyakhovetskii V, Tondera C, Gorsky O, Moosavi S, et al. Rapid prototyping of soft bioelectronic implants for use as neuromuscular interfaces. *Nat Biomed Eng* 2020;4:1010–22. <https://doi.org/10.1038/s41551-020-00615-7>.
- [18] Kaur G, Adhikari R, Cass P, Bown M, Gunatillake P. Electrically conductive polymers and composites for biomedical applications. *RSC Adv* 2015;5:37553–67. <https://doi.org/10.1039/C5RA01851J>.
- [19] van den Brand R, Heutschi J, Barraud Q, DiGiovanna J, Bartholdi K, Huerlimann M, et al. Restoring voluntary control of locomotion after paralyzing spinal cord injury. *Science* 2012;336:1182–5. <https://doi.org/10.1126/science.1217416>.
- [20] Moretto H-H, Schulze M, Wagner G. Silicones. Wiley-VCH Verlag GmbH & Co. KGaA. In: *Ullmann's encyclopedia of industrial chemistry*. Weinheim, Germany: Wiley-VCH Verlag GmbH & Co. KGaA; 2000. https://doi.org/10.1002/14356007.a24_057. a24_057.
- [21] Deriabin KV, Lobanovskaia EK, Kirichenko SO, Barshutina MN, Musienko PE, Islamova RM. Synthesis of ferrocenyl-containing silicone rubbers via platinum-catalyzed Si–H self-cross-linking. *Appl Organomet Chem* 2020;34:e5300. <https://doi.org/10.1002/aoc.5300>.
- [22] Deriabin KV, Yaremenko IA, Chislov MV, Fleury F, Terent'ev AO, Islamova RM. Similar nature leads to improved properties: cyclic organosilicon triperoxides as promising curing agents for liquid polysiloxanes. *New J Chem* 2018;42:15006–13. <https://doi.org/10.1039/C8NJ02499E>.
- [23] Dobrynin MV, Pretorius C, Kama DV, Roodt A, Boyarskiy VP, Islamova RM. Rhodium(I)-catalysed cross-linking of polysiloxanes conducted at room temperature. *J Catal* 2019;372:193–200. <https://doi.org/10.1016/j.jcat.2019.03.004>.
- [24] Plevová K, Mudráková B, Šebesta R. A practical three-step synthesis of vinylferrocene. *Synthesis* 2018;50:760–3. <https://doi.org/10.1055/s-0036-1589142>.
- [25] Yilmaz B, Pazarcevirin AE, Tezcaner A, Evis Z. Historical development of simulated body fluids used in biomedical applications: a review. *Microchem J* 2020;155:104713. <https://doi.org/10.1016/j.microc.2020.104713>.
- [26] Gerasimenko Y, Musienko P, Bogacheva I, Moshonkina T, Savochin A, Lavrov I, et al. Propriospinal bypass of the serotonergic system that can facilitate stepping. *J Neurosci* 2009;29:5681–9. <https://doi.org/10.1523/JNEUROSCI.6058-08.2009>.
- [27] Shik ML, Severin FV, Orlovskii GN. Control of walking and running by means of electric stimulation of the midbrain. *Biofizika* 1966;11:659–66.
- [28] Braga SS, Silva AMS. A new age for iron: antitumoral ferrocenes. *Organometallics* 2013;32:5626–39. <https://doi.org/10.1021/om400446y>.
- [29] Ornelas C. Application of ferrocene and its derivatives in cancer research. *New J Chem* 2011;35:1973. <https://doi.org/10.1039/c1nj20172g>.
- [30] van Staveren DR, Metzler-Nolte N. Bioorganometallic chemistry of ferrocene. *Chem Rev* 2004;104:5931–86. <https://doi.org/10.1021/cr0101510>.
- [31] Hartinger CG, Metzler-Nolte N, Dyson PJ. Challenges and opportunities in the development of organometallic anticancer drugs. *Organometallics* 2012;31:5677–85. <https://doi.org/10.1021/om300373t>.
- [32] Sandalcioğlu IE, Gasser T, Asgari S, Lazorisak A, Engelhorn T, Egelhof T, et al. Functional outcome after surgical treatment of intramedullary spinal cord tumors: experience with 78 patients. *Spinal Cord* 2005;43:34–41. <https://doi.org/10.1038/sj.sc.3101668>.
- [33] Hoffman P. Beiträge zur Kenntnis der menschlichen Reflexe mit besonderer Berücksichtigung der elektrischen Erscheinungen. *Arch F Physiol* 1910;1:223–56.
- [34] Capogrosso M, Wenger N, Raspopovic S, Musienko P, Beauparlant J, Bassi Luciani L, et al. A computational model for epidural electrical stimulation of spinal sensorimotor circuits. *J Neurosci* 2013;33:19326–40. <https://doi.org/10.1523/JNEUROSCI.1688-13.2013>.
- [35] Shkhorbatova P, Lyakhovetskii V, Pavlova N, Popov A, Bazhenova E, Kalinina D, et al. Mapping of the spinal sensorimotor network by transvertebral and transcutaneous spinal cord stimulation. *Front Syst Neurosci* 2020;14:555593. <https://doi.org/10.3389/fnsys.2020.555593>.